ELSEVIER

Carbohydrate Research 278 (1995) 205–225

CARBOHYDRATE RESEARCH

A conformational model for cyclic β-(1 → 2)-linked glucans based on NMR analysis of the β-glucans produced by *Xanthomonas campestris*

William S. York

Complex Carbohydrate Research Center, The University of Georgia, 220 Riverbend Road, Athens, GA 30602-4712, USA

Received 30 May 1995; accepted 5 July 1995

Abstract

A cyclic hexadecaglucoside containing 15 β-(1 → 2)-linkages and one α-(1 → 6)-linkage {A. Amemura and J. Cabrera-Crespo, *J. Gen. Microbiol.* 132 (1986) 2443–2452} was purified from cultures of *Xanthomonas campestris*. The homogeneity of this glucan preparation facilitated the complete assignment of its ^{1}H NMR spectrum and the assignment of all of the C-1 and C-2 resonances in its ^{13}C NMR spectrum to specific residues within the glucan. The resonances (i.e., H-1, H-2, C-1 and C-2) that are closely associated with the β-(1 → 2) glycosidic bonds of this glucan are dispersed over a relatively broad chemical shift range. This chemical shift dispersion is attributed to the differences in the time-averaged geometry of individual β-(1 → 2)-linked glycosidic bonds in this glucan and is consistent with the hypothesis that these glycosidic bonds have less conformational freedom than do the glycosidic bonds in a linear β-(1 → 2)-linked glucan. The chemical shifts of H-1, H-2, C-1, and C-2 exhibit an alternating pattern when plotted as a function of their locations within the macrocyclic ring, suggesting that the glycosidic bond geometry also alternates in the glucan. A new conformational model for cyclic β-(1 → 2)-linked glucans was developed on the basis of these observations. This model is consistent with the observed spectroscopic features of all cyclic β-(1 → 2)-linked glucans known to be produced by Gram-negative bacteria.

Keywords: Hexadecaglucoside, cyclic; *Xantohomonas campestris*; Glucan; Model, conformational

SSDI 0008-6215(95)00260-X

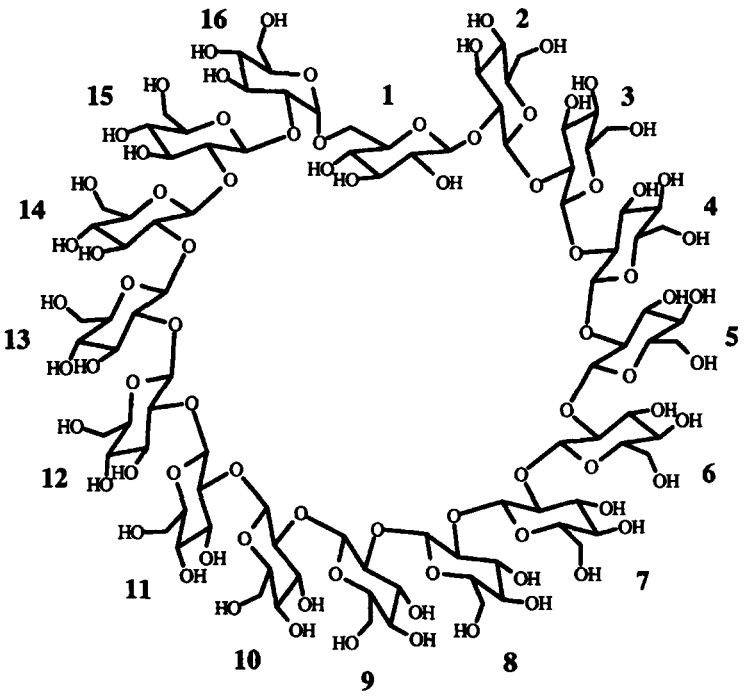

Fig. 1. Chemical structure of the most abundant cyclic β-glucan, α-cyclosophorohexadecaose (α-C16), produced in culture by *Xanthomonas campestris*. Throughout this manuscript, each of the 16 β-Glc*p* residues in α-C16 is identified by a number, as depicted in this Fig. The α-(1 → 6)-linkage between residues **16** and **1** gives α-C16 its unique spectroscopic characteristics, compared to the cyclic β-glucans produced by the Rhizobiaceae, which contain from 17 to 40 Glc*p* residues, all of which are β-(1 → 2)-linked.

1. Introduction

Many species of Gram-negative bacteria produce low-molecular-weight β-glucans that are sequestered in the periplasmic space [1,2]. It has been proposed that an important function of these β-glucans is to maintain the osmotic potential of the periplasm, thereby enabling the bacterium to adapt to variations in the osmotic potential of its environment [1]. Bacteria of the genera *Agrobacterium* and *Rhizobium* produce periplasmic glucans, referred to as cyclosophorans, that contain from 17 to 40 β-(1 → 2)-linked Glc*p* residues [3] that form a covalently closed macrocycle [4]. Bacteria of the genus *Xanthomonas* also produce a unique cyclic β-glucan that contains only 16 Glc*p* residues, 15 of which are β-linked to C-2 of the next residue and one of which is α-linked to C-6 of the next residue (Fig. 1) [5]. The spectroscopic analysis of this molecule, α-cyclosophorohexadecaose (α-C16), is the primary focus of this paper.

Several conformational models for the cyclosophorans produced by the Rhizobiaceae have been proposed on the basis of conformational energy calculations [6–8]. A feature common to all of these models is the requirement, at any given instant in time, that the glycosidic bond conformation must vary from residue to residue. A cyclic glucan can be

considered a helical structure in which the number of residues per turn is an integer and the helix pitch is zero [6]. However, when $\phi_1 = \phi_2 = \ldots = \phi_n$ and $\psi_1 = \psi_2 = \ldots = \psi_n$, these criteria are not fulfilled by any single energetically accessible glycosidic bond conformation (defined by the torsional angles ϕ = H-1–C-1–O-2′–C-2′, ψ = C-1–O-2′–C-2′–H-2′) [6]. Therefore, it was proposed that cyclosophoran structures embody repeating conformational subunits composed of three [6], four [7], or seven [7] sugar residues, wherein ($\phi_i = \phi_{i+3}$ and $\psi_i = \psi_{i+3}$), ($\phi_i = \phi_{i+4}$ and $\psi_i = \psi_{i+4}$), and ($\phi_i = \phi_{i+7}$ and $\psi_i = \psi_{i+7}$), respectively. Less symmetrical models based on combinations of more than one such conformational subunit [7] or on an alternating sequence of glycosidic bond conformations [8] have also been suggested.

Analysis of the molecular conformations of glycans is particularly challenging due to the high flexibility of the glycosidic linkage [9,10]. This flexibility increases the entropic cost of crystallization, making it difficult to obtain crystals that are adequate for diffraction studies. Spectroscopic analysis of the conformations of glycans in solution can be complicated by the simultaneous existence of a large number of energetically accessible conformers, which often interconvert on the microsecond or faster time scale [9]. Thus, the inherent flexibility of most glycans makes it extremely difficult to obtain a realistic description of their preferred conformational states.

It is probable that the macrocyclic structure of some periplasmic β-glucans imposes constraints on the conformational states adopted by these molecules. Such constraints may significantly simplify the conformational analysis of these glucans and may also endow them with unique physical properties. For example, cyclodextrins [11,12], which are macrocyclic α-(1 → 4)-linked glucans that usually contain from six to eight Glc*p* residues, have been widely reported to form inclusion complexes with a variety of nonpolar guest molecules. The molecular conformations of cyclodextrins and their inclusion complexes with various ligands have been widely studied by spectroscopic [11] and diffraction [12] techniques. However, the molecular conformations of the cyclic β-(1 → 2)-glucans have not been experimentally established.

The macrocyclic structure of the cyclosophorans produced by Rhizobiaceae leads to several interesting consequences with regard to the spectral properties of these molecules. All the Glc*p* residues of a Rhizobiaceae cyclosophoran are β-(1 → 2)-linked, and the lack of terminal residues makes every glucosyl residue in the cyclosophoran chemically equivalent. However, all of the proposed conformational models predict that various glucosyl residues within the cyclic glucan are in different microenvironments at any given instant [6–8]. Nevertheless, only six ^{13}C resonances (C-1 through C-6, Fig. 2) and seven ^{1}H resonances (H-1 through H-6′, Fig. 2) are observed in the NMR spectra of a size-homogeneous cyclosophoran [7,13]. This experimental result indicates that, on the NMR time scale, each glucosyl residue in the cyclosophoran experiences the same average microenvironment. This observation can be reconciled with conformational energy calculations for cyclosophorans only if the microenvironments of individual glucosyl residues are assumed to interconvert rapidly in solution.

The rapid conformational interconversion and the resulting magnetic equivalence of the glucosidic residues of a cyclosophoran makes it experimentally difficult to distinguish the interactions (i.e., scalar and dipolar coupling) of two magnetic nuclei that reside within a single residue from the interactions of nuclei that reside in different

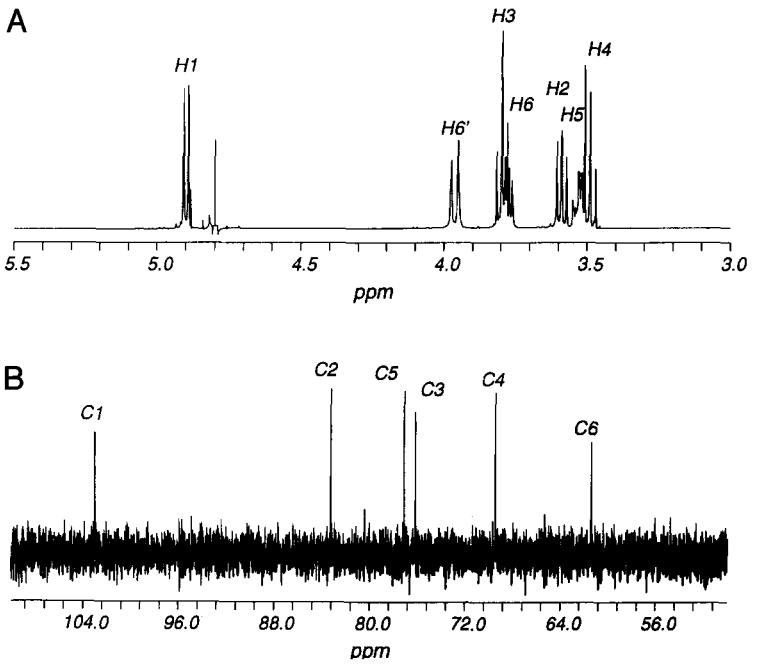

Fig. 2. (A) ^{1}H NMR spectrum of the purified cyclosophoran consisting of 19 β-(1 → 2)-linked Glc$p$ residues. The minor signals upfield of the H-1 resonance (δ 4.9) are due to HDO. (B) ^{13}C NMR spectrum of the same cyclosophoran. The simplicity of these spectra (compare Fig. 3) is probably due to conformational averaging of the environments of the 19 Glc$p$ residues in this molecule.

residues [13]. Thus, information regarding glycosidic bond geometry of a cyclosophoran can be obtained only by techniques [13], such as the use of a dilute spin-label, that allow individual glycosidic residues to be distinguished due to differences in their magnetic environments. Furthermore, NMR generally can only provide information about the time-averaged geometry of molecules that undergo rapid conformational interconversion [14]. Therefore, a cyclic glucan that exhibits a high degree of conformational constraint would be an attractive model compound for conformational analysis by NMR.

The NMR spectra of α-C16 are more complex than the spectra of cyclic β-(1 → 2) glucans produced by the Rhizobiaceae. The relatively small size of the α-C16 macrocyclic ring and the presence of a single α-(1 → 6)-linkage in its structure impose a unique magnetic environment upon each of the 15 β-Glc$p$ residues in the molecule [5]. This condition allows intraresidue magnetic interactions to be distinguished from interresidue interactions, and thus makes it possible to probe the individual glycosidic bond conformations of α-C16 by NMR spectroscopy. The complete assignment of the ^{1}H NMR spectrum of α-C16 is presented herein, along with evidence that the conformation of this unique cyclic glucan is more constrained than that of the cyclosophorans produced by the Rhizobiaceae. The chemical shift effects that arise from these constraints are interpreted in terms of a general conformational model for β-(1 → 2)-linked glucans that can account for their cyclic structure and dynamic properties.

2. Experimental

Purification of α-C16.—Xanthomonas campestris pv. glycines (PDDCC 7414) was cultured in 1.5 L of the medium described by Higashiura et al. [15]. Ethanol (100%, 3 L) was added to the 6-day-old culture and mixed thoroughly. The resulting precipitate and cell debris were removed by centrifugation at 5000 rpm in a Beckman JA-10 rotor. The supernatant solution was decanted, thoroughly mixed with ethanol (100%, 12 L), and chilled (4°C, 12 h). The resulting precipitate was collected by centrifugation at 7000 rpm in the JA-10 rotor, dissolved in 250 mL of water, filtered through a nylon membrane (0.2 μm pore, Nalgene), and dialyzed against deionized water (2 × 30 L) in 1000 MWCO tubing (Spectra/Por 6). Anionic contaminants were removed by passing the retentate through a 2 × 5 cm column containing QAE-Sephadex A-25 (Sigma) equilibrated with water. The eluant containing the β-(1 → 2) glucans was lyophilized and redissolved in 5.0 mL of water. An aliquot (1.5 mL) of this solution was loaded onto a 90 × 1.6 cm column of Bio-Gel P-2 (−400 mesh, Bio-Rad) and eluted with deionized water. Fractions (60 drops, 2.0 mL) were collected and assayed colorimetrically for hexose content. Fractions 26 and 27 gave the highest colorimetric response and were also the most enriched in α-C16, as determined by MALD-TOF MS analysis (see below). These two fractions were separately carried through the remaining purification steps, and the α-C16 obtained from them was pooled only after the final high-pH anion-exchange chromatography step (see below).

Individually lyophilized P-2 fractions 26 and 27 were each redissolved in 500 μL of HPLC-grade water and injected (125 μL per injection) on a 1.0 × 25 cm octadecylsilica column (Hibar Lichrosorb RP-18) eluted with 96.5:3.5 water–methanol. When either P-2 fraction 26 or 27 was injected, the largest peak (t_R 19 min) detected by monitoring the refractive index of the ODS eluant contained α-C16 as its dominant component. The material that eluted at 19 min was dried, and the residue was dissolved in water (300 μL per P-2 fraction) and further purified by high-performance anion-exchange chromatography (HPAEC) as follows. Aliquots (6 × 50 μL for each P-2 fraction) were injected on a Dionex CarboPac PA1 column (4 × 250 mm) and eluted with 80 mM NaOAc in 100 mM NaOH for 5 min, followed by a linear gradient (80 to 350 mM NaOAc in 100 mM NaOH, over 30 min) at a flow rate of 1.0 mL/min. Essentially homogeneous α-C16 (t_R ~ 15 min, ~ 5 mg total) was detected by voltage-pulsed amperometry. HPAEC fractions were neutralized with CO_2 gas, loaded onto a column of graphitized carbon (Alltech Graphtrap-GB, 0.2 mL matrix per mL HPAEC eluant) that was preconditioned with 100% acetonitrile, 50% aqueous acetonitrile, and then water (> 25 column volumes of each). Salts were eluted from the column with water (5 column volumes), and salt-free glucans were then eluted with 25% and 50% aqueous acetonitrile (5 column volumes of each).

Purification of Rhizobiaceae cyclosophorans.—Size-homogeneous cyclic glucans consisting entirely of β-(1 → 2)-linked Glc*p* residues were isolated [13] from the culture fluid of strain ANU 437 of *Rhizobium trifolii* by anion-exchange and reversed-phase chromatography [3].

Matrix-assisted laser-desorption time of flight spectrometry (MALD-TOF).—Aqueous solutions (5 μL, ~ 1 μg/μL) of glucans were mixed with an equal volume of 100

mM 2,4-dihydroxybenzoic acid in 9:1 water–MeOH. Approximately 1 μL of this mixture was applied to the MALD probe and dried under vacuum. MALD-TOF spectra were recorded with a Hewlett–Packard (LDI 1700 XP) TOF spectrometer operating at 30 kV accelerating voltage and a pressure of 0.4×10^{-6} to 1.1×10^{-6} torr. Ion desorption was accomplished with a nitrogen laser ($\lambda = 337$ nm) with a pulse width of 3 ns and an average laser energy of ~ 10 μJ per pulse.

NMR spectroscopy.—Solutions of the purified glucans in deuterium oxide (99.6 atom % ^{2}H, Cambridge Isotope Laboratories, CIL) were lyophilized to remove exchangeable protons, and the residues were dissolved in D_2O (99.96% atom % ^{2}H, CIL). ^{1}H NMR spectra and heteronuclear (two-dimensional) spectra were recorded at 302 K with a Bruker AMX 600 spectrometer. Proton-decoupled ^{13}C NMR spectra were recorded with a Bruker AM 500 spectrometer. All two-dimensional spectra (double-quantum filtered COSY [16], TOCSY [17], NOESY [18], and HSQC [19,20]) were recorded using the time-proportional phase increment (TPPI) method [21] in both dimensions. HSQC spectra were recorded with GARP decoupling [22] of ^{13}C during the acquisition period (t_2). *J* cross-peaks (ZQC artifacts) in the NOESY spectrum were shifted out of the H-1–H-2 cross-peak region by incrementing the ZQC evolution time τ_i by a fraction χ of the t_1 increment while maintaining a constant mixing time τ_m [18]. This was accomplished with the following pulse sequence [18] $\{\pi/2 \ldots t_1 \ldots \pi/2 \ldots \Delta_1 \ldots \pi \ldots \Delta_2 \ldots \pi/2 \ldots \text{Acq}\}$, where $\tau_m = \Delta_1 + \Delta_2$ and $\tau_i = \tau_m - (2 \times \Delta_2)$. The delay Δ_1 was incremented by 55.4 μs, and the delay Δ_2 was decremented by 55.4 μs, thus incrementing τ_i by 110.8 μs for successive values of t_1. This corresponds to a value of ~ 0.44 for χ (the t_1 increment being 252 μs), which shifts the H-1–H-2 *J* cross-peaks into two areas of the spectrum that are devoid of NOESY cross-peaks (i.e., in ω_1, between the crowded envelope of ring protons and the anomeric protons, and downfield from the anomeric protons), and makes it unnecessary to suppress *J* cross-peaks by variation of τ_m. The total NOESY mixing time was 250 ms.

Conformational energy calculations.—Conformational energy calculations were performed as previously described [7]. The HSEA approach as implemented in the GEGOP program [23] was used to perform the Monte Carlo simulation (Fig. 6), and SYBYL 6.1 (Tripos Associates, St. Louis, MO) with the standard Tripos force field was used to perform energy minimizations and thereby assess the steric accessibility of specific β-(1 → 2) glucan conformations (Fig. 8 and Table 3). A typical simulated annealing was performed via a series of 1-ps MD simulations in which the temperature parameter was decreased from 100 to 10 K in steps of 30 K. It should be noted that neither of the force fields used provides a realistic picture of the energetics of the system, because, for example, solvent, hydrogen bonding, and electrostatic terms were not included. However, these computational approaches can adequately determine whether a conformation is sterically forbidden, which was the primary goal of these initial calculations.

3. Results and discussion

Purification and chemical structure of β-glucans.—Homogeneous preparations of several glucans were obtained from liquid cultures of the bacterium *Xanthomonas*

Table 1
^{1}H Resonance [a] assignments for α-cyclosophorohexadecaose (α-C16)

Position [b]	H-1	H-2	H-3	H-4	H-5	H-6	H-6′
1	4.916	3.330	3.539	3.383	3.748	3.866	3.866
2	4.810	3.721	3.784	3.436	3.53	3.80	3.976
3	4.979	3.532	3.724	3.489	3.50	3.764	3.951
4	4.883	3.646	3.854	3.514	3.536	3.823	3.948
5	5.003	3.541	3.774	3.471	3.50	3.757	3.958
6	4.834	3.668	3.81	3.475	3.52	3.80	3.952
7	5.047	3.576	3.760	3.518	3.50	3.760	3.946
8	4.857	3.704	3.813	3.464	3.511	3.779	3.951
9	4.925	3.586	3.750	3.534	3.53	3.798	3.944
10	5.003	3.614	3.797	3.460	3.506	3.756	3.957
11	4.815	3.681	3.815	3.486	3.515	3.806	3.945
12	5.022	3.536	3.760	3.50	3.50	3.772	3.959
13	4.852	3.686	3.818	3.480	3.51	3.780	3.951
14	4.931	3.552	3.775	3.53	3.53	3.845	3.961
15	4.663	3.643	3.780	3.493	3.46	3.754	3.912
16	5.172	3.632	3.962	3.528	3.717	3.790	3.883
Statistics for β-Glcp residues 3–14							
Minimum	4.815	3.532	3.724	3.460	3.500	3.756	3.944
Maximum	5.047	3.704	3.854	3.534	3.536	3.845	3.961
Range	0.232	0.172	0.130	0.074	0.036	0.089	0.017
Mean	4.929	3.610	3.787	3.493	3.513	3.787	3.952
σ (N) [c]	0.077	0.062	0.035	0.024	0.013	0.027	0.005

[a] Chemical shifts in ppm relative to internal acetone (δ 2.225).
[b] Residues are numbered starting with the 6-substituted β-Glc*p* residue, as shown in Fig. 1.
[c] Root mean square deviation.

campestris [5]. The previously described purification procedure [5] results in preparations that are mixtures of linear and cyclic glucans, and so a new procedure was developed utilizing size-exclusion chromatography, reversed-phase chromatography, and high-performance ion-exchange chromatography (see Experimental).

The primary structure of the most abundant glucan produced in culture by *Xanthomonas* is depicted in Fig. 1. This structure, α-cyclosophorohexadecaose (α-C16), was previously proposed by Amemura and Crabera-Crespo [5], and is consistent with the analytical data obtained in the present study (Tables 1 and 2). Analysis of the ^{1}H NMR spectrum (Fig. 3) of α-C16 that was obtained via the improved purification procedure indicated that it is homogeneous. The availability of homogeneous α-C16 made it possible to make residue-specific assignments of all 112 resonances in its ^{1}H NMR spectrum (Table 1) and all of the C-1 and C-2 resonances (Table 2) in its ^{13}C NMR spectrum.

The ^{1}H NMR spectrum of α-C16.—Each Glc*p* residue of α-C16 constitutes an isolated, *J*-coupled (^{1}H) spin sytem. It was possible to extract ^{1}H NMR subspectra for nearly all residues by taking cross-sections of the TOCSY spectrum (not shown) through diagonal peaks corresponding to the anomeric proton resonances (δ 5.172–4.663). Extraction of the cross-section through the (degenerate) anomeric resonances of residues

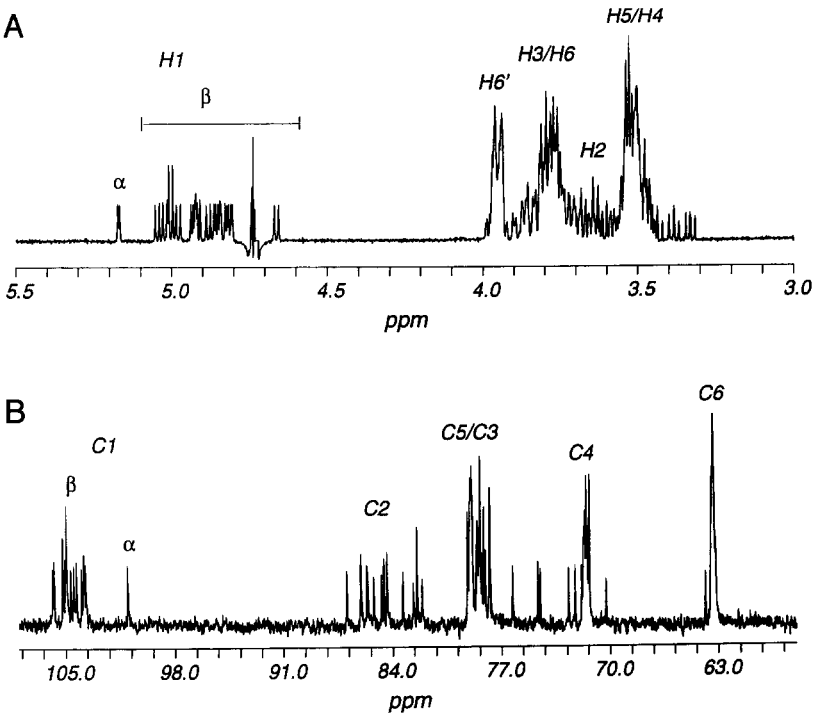

Fig. 3. (A) ^{1}H NMR spectrum of α-C16, whose structure is shown in Fig. 1. Baseline distortion and signals at δ 4.73 are due to HDO. (B) ^{13}C NMR spectrum of α-C16. The relative complexity of these spectra, compared to the spectra of cyclosophorans produced by the Rhizobiaceae (Fig. 2) is attributed to conformational constraint and other factors (see text). Resonance assignments for α-C16 are given in Tables 1 and 2.

5 and **10** (δ 5.003) yielded a subspectrum corresponding to the sum of these residues. However, a clean subspectrum of residue **5** was extracted by taking the TOCSY cross-section through its H-2 diagonal peak (δ 3.614). Comparison of the cross-sections through the diagonal peaks at δ 5.003 and δ 3.614 allowed the resonances of residues **5** and **10** to be distinguished. Analysis of TOCSY cross-sections allowed every resonance in the ^{1}H NMR spectrum of α-C16 to be assigned to a specific proton in a specific spin-system, but did not provide the information necessary to assign each spin-system to a specific Glc*p* residue.

Analysis of the COSY (Fig. 4) and NOESY (Fig. 5) spectra of α-C16 led to the assignment of resonances to individual Glc*p* residues in the molecule. The transdiaxial orientation of H-1 and H-2 in β-Glc*p* residues leads to a large H-1–H-2 scalar coupling constant ($^3J_{1,2}$ 8 Hz) and subsequently to strong H-1–H-2 cross-peaks in the COSY spectrum of α-C16 (Fig. 4). This sugar geometry also places these two nuclei at a distance (approximately 3 Å apart) that is too great to result in observable intraglycosidic H-1–H-2 NOESY cross-peaks under the experimental conditions employed. However, an interglycosidic H-1–H-2′ cross-peak was observed for every β-(1 → 2)-linkage in the molecule, indicating that every β-(1 → 2)-linked glycosidic bond in α-C16 adopts

Table 2
^{13}C Resonance assignments [a] for α-cyclosophorohexadecaose (α-C16)

Position [b]	C-1	C-2	C-3	C-4	C-5	C-6
1	105.04	76.29	III [c]	72.70	V [c]	70.28
2	105.72	83.36	III [c]	72.29	V [c]	63.86
3	104.30	86.95	III [c]	IV [c]	V [c]	VI [c]
4	104.96	84.38	III [c]	IV [c]	V [c]	VI [c]
5	103.85	85.66	III [c]	IV [c]	V [c]	VI [c]
6	104.66	82.69	III [c]	IV [c]	V [c]	VI [c]
7	103.82	85.61	III [c]	IV [c]	V [c]	VI [c]
8	104.91	82.12	III [c]	IV [c]	V [c]	VI [c]
9	104.49	85.22	III [c]	IV [c]	V [c]	VI [c]
10	103.71	84.38	III [c]	IV [c]	V [c]	VI [c]
11	105.17	82.44	III [c]	IV [c]	V [c]	VI [c]
12	103.99	86.03	III [c]	IV [c]	V [c]	VI [c]
13	105.18	82.44	III [c]	IV [c]	V [c]	VI [c]
14	104.96	86.06	III [c]	IV [c]	V [c]	VI [c]
15	105.81	84.72	III [c]	IV [c]	V [c]	VI [c]
16	101.04	84.56	74.52	71.8	74.67	63.4
Statistics for β-Glcp residues 3–14						
Minimum	103.71	82.12	77.65 [d]	71.86 [d]	79.20 [d]	63.51 [d]
Maximum	105.18	86.95	78.73 [d]	71.36 [d]	78.88 [d]	63.20 [d]
Range	1.47	4.83	1.08 [d]	0.50 [d]	0.32 [d]	0.31 [d]
Mean	104.50	84.50	78.17 [d]	71.60 [d]	79.01 [d]	63.40 [d]
σ (N) [e]	0.53	1.62	0.35 [d]	0.15 [d]	0.11 [d]	0.10 [d]

[a] Chemical shifts in ppm relative to internal acetone (δ 33.02).
[b] Residues numbered as in Fig. 1.
[c] Most of the C-3 through C-6 resonances could only be assigned to one of several clusters of unresolved resonances. The locations of these clusters within the spectrum correspond to the limits given in the bottom part of the Table. Cluster III corresponds to C-3, Cluster IV to C-4, etc. Clusters I and II contain the resolved C-1 and C-2 resonances, respectively.
[d] The statistics indicated were performed on signal clusters, and may thus include resonances of residues **1**, **2**, **15**, and **16**.
[e] Root mean square deviation.

a geometry that brings H-1 to within 3 Å of H-2′, at least transiently. This set of conditions made it possible to trace the alternating dipolar and scalar connectivity from H-1 of the 6-linked β-Glc*p* residue **1** completely around the macrocyclic ring of α-C16 back to H-6 of residue **1**, thus assigning each of the isolated spin-systems of this glucan to a specific Glc*p* residue.

The ^{1}H NMR assignments described above were completely consistent with the structure (Fig. 1) originally proposed by Amemura et al. [5]. The presence of the α-(1 → 6)-linkage in α-C16 produces several chemical shift effects that warrant some comment. β-Glc*p* **1** (Fig. 1) does not bear a glucosyl substituent at O-2, and consequently its H-2 resonance (δ 3.330) is shifted significantly upfield relative to the H-2 resonances of the other 14 β-Glc*p* residues (δ 3.532–3.721, Table 1). This chemical shift effect is typical for O-2 glycosylation of β-Glc*p* residues [24]. The H-5 resonance

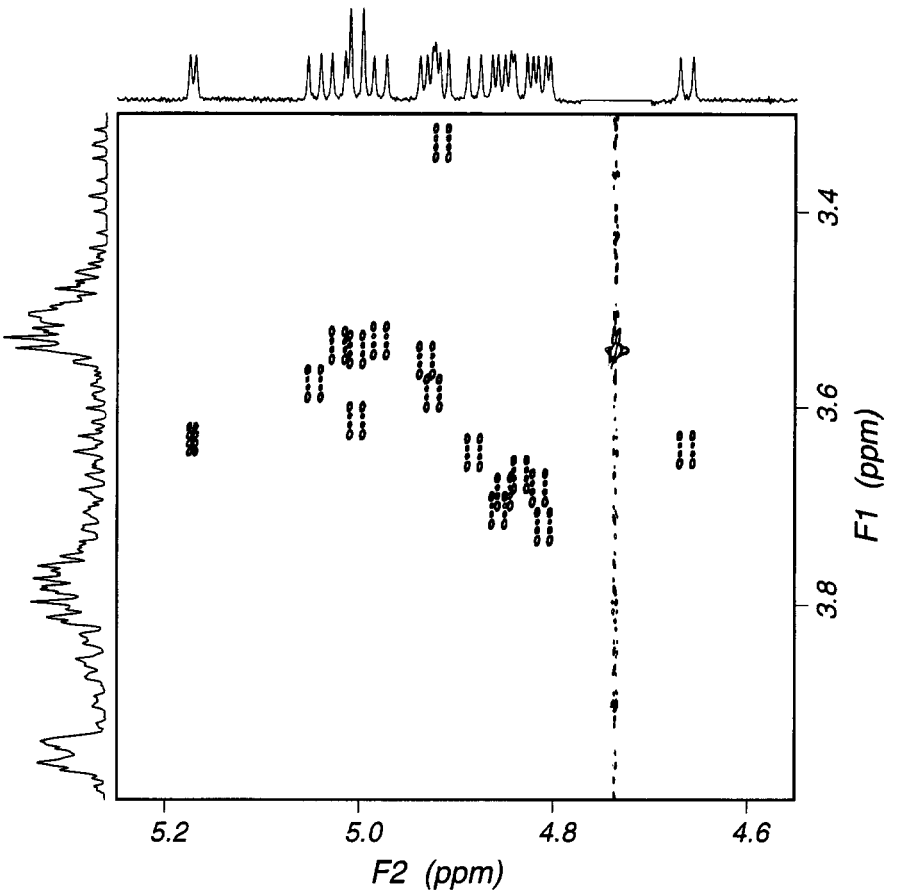

Fig. 4. H-1–H-2 cross-peak region of the COSY spectrum of α-C16. Each of the 16 residues of α-C16 give rise to a H-1–H-2 cross-peak that is easily distinguished in the 2D plot. These cross-peaks correspond to the scalar interaction between H-1 and H-2 within each residue.

of β-Glc*p* **1** (δ 3.748) is deshielded relative to the H-5 resonances of the other β-Glc*p* residues (δ 3.46–3.54, Table 1) due to the presence of an α-Glc*p* at O-6. This shift is expected because the H-5 resonance of a β-Glc*p* residue with an α-pyranosyl residue (D-*gluco* configuration) attached at O-6 is typically deshielded by approximately 0.2 ppm relative to an otherwise equivalent unsubstituted β-Glc*p* residue [25,26]. β-Glc*p* **15** is glycosidically linked to O-2 of α-Glc*p* **16** rather than to a β-Glc*p* residue, and so its H-1 resonance (δ 4.663) is upfield relative to the other β-anomeric resonances (δ 4.810–5.047, Table 1) of α-C16. An analogous chemical shift effect is observed in the ^{1}H NMR spectra of the two mutarotational isomers of the reducing disaccharide sophorose, wherein H-1 of the non-reducing β-Glc*p* residue (δ 4.624) in α-sophorose is 0.159 ppm upfield of H-1 of the analogous non-reducing β-Glc*p* residue (δ 4.783) in β-sophorose. Thus, the effects of the α-(1 → 6)-linkage on the chemical shifts of

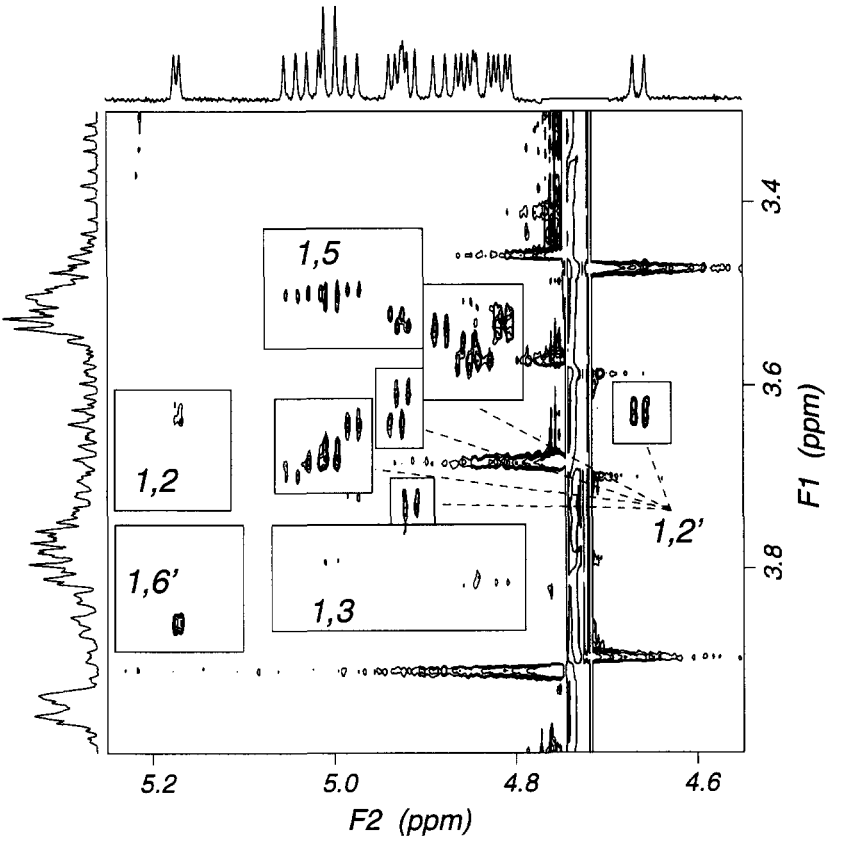

Fig. 5. Region of the NOESY spectrum of α-C16, covering the same frequency limits as shown for the COSY spectrum in Fig. 4. The H-1–H-2 cross-peak for the α-Glc*p* residue, and H-1–H-3 and H-1–H-5 cross-peaks for the β-Glc*p* residues arise from the dipolar (through-space) interactions within residues. The H-1–H-6′ cross-peak and the H-1–H-2′ cross-peaks arise from dipolar interactions between Glc*p* residues linked by the α-(1 → 6) linkage and the β-(1 → 2) linkages, respectively. The combined NOESY and COSY (Fig. 4) data allows each of the H-1 and H-2 resonances to be assigned to a specific Glc*p* residue within α-C16 (Table 1).

protons of nearby β-Glc*p* residues of α-C16 are consistent with observations for other glycans with analogous structural features.

The ^{13}C NMR spectrum of α-C16.—Resonances in the ^{13}C NMR spectrum of α-C16 (Fig. 3B) were assigned (Table 2) by one-bond heteronuclear correlation spectroscopy in the form of a 2D HSQC experiment [19]. The ^{1}H NMR assignments of α-C16 (described above) made it possible to assign all ^{13}C resonances for the α-Glc*p* residue, and all C-1 and C-2 resonances for the β-Glc*p* residues. Four other resonances that are resolved in the ^{13}C NMR spectrum of α-C16 were assigned to β-Glc*p* residues **1** and **2**, which have atypical environments due to their proximity to the α-linked Glc*p* residue. Specifically, C-4 and C-6 of β-Glc*p* **1** are resolved because this residue is substituted at O-6 with an α-Glc*p* residue, rather than at O-2 with a β-Glc*p* residue. The presence of

a glucosyl substituent at O-2 of β-Glc*p* residues **2–15** introduces an additional steric constraint on the conformational freedom of each of the β-(1 → 2) glycosidic bonds linking these residues to their aglycons (residues **3–16**). The locally imposed constraints on the geometry of the β-(1 → 2) linkage between residues **1** and **2** are unique because β-Glc*p* **1** does not have a substituent at O-2. This condition facilitates the assignment of the C-4 and C-6 resonances of residue **2** by shifting them away from the C-4 and C-6 resonances of other β-Glc*p* residues of α-C16.

Is α-C16 conformationally constrained?—The cyclosophorans produced by the Rhizobiaceae, which are composed entirely of β-(1 → 2)-linked Glc*p* residues, give rise to very simple ^{1}H NMR (Fig. 2A) and ^{13}C NMR (Fig. 2B) spectra. The smallest cyclosophoran produced by the Rhizobiaceae consists of a 17-residue macrocycle [2], and smaller rings are apparently precluded by steric constraints. Although no model exists that allows all of the β-(1 → 2) glycosidic bonds of a cyclosophoran of this type to simultaneously adopt the same conformation (see Introduction), all of the β-Glc*p* residues of a size-homogeneous cyclosophoran are magnetically equivalent, resulting in a ^{1}H NMR spectrum (Fig. 2A) that contains only seven resonances (H-1–H-6′) and a ^{13}C NMR spectrum (Fig. 2B) that contains only six resonances (C-1–C-6). This signal degeneracy is probably due to the rapid (on the NMR time scale) [14] interconversion of glycosidic bond geometries.

In contrast, the resonances of individual glucosyl residues can be readily distinguished in the ^{1}H and ^{13}C NMR spectra of α-C16 (Figs. 3–5). Several factors may lead to the greater chemical shift dispersion exhibited by the resonances of α-C16, compared to the cyclosophorans produced by Rhizobiaceae. Differences in the proximity and orientation of each β-Glc*p* residue with respect to the α-linked residue in α-C16 are likely to affect their chemical shifts via anisotropic shielding effects. However, conformational constraint could also produce chemical shift effects by imposing different geometric constraints on each β-(1 → 2) linkage in the ring, placing each β-Glc*p* residue in a different magnetic environment.

The H-1, H-2, C-1, and C-2 resonances of α-C16 exhibit significantly greater chemical shift dispersion than do the other resonances of this glucan (Tables 1 and 2). The chemical shifts of the ^{13}C resonances that are directly involved in the glycosidic linkage are far more sensitive to differences in the glycosidic bond conformation (i.e., the dihedral angles ϕ and ψ) than are other carbon atoms [27]. Therefore, constraints that impose a different (average) glycosidic bond geometry upon each β-(1 → 2) linkage in α-C16 would result in greater chemical shift dispersion for C-1 and C-2 than for C-3 through C-6, making the statistics given in Table 2 consistent with the existence of such constraints. (Note that these chemical shift statistics do not include residues **1**, **2**, **15**, and **16**, whose resonances may be more strongly affected by direct interaction with the nearby α-(1 → 6)-linkage.) It is possible that the glycosyl residues of α-C16 happen to be situated such that direct (through-space) shielding effects of the α-(1 → 6)-linkage are consistently larger for C-1 and C-2 than for other carbon atoms in these residues. However, it is more likely that conformational constraints are the dominant factors leading to the differences in chemical shift dispersion described above. Similar arguments can be made on the basis of the greater chemical shift dispersion of the H-1 and H-2 resonances of α-C16 compared to those of H-3 through H-6′ (Table 1).

Implications for conformational models of cyclic β-(1 → 2)-glucans.—Although the broad chemical shift dispersion in the ^{1}H and ^{13}C spectra of α-C16 can be interpreted as a manifestation of differences in the average geometry of individual glycosidic bonds, this does not imply that α-C16 is a rigid molecule. Conformational constraints may disfavor certain combinations of glycosidic bond geometry in α-C16. Such constraints could limit the time that a given glycosidic bond spends in a particular conformation, but still allow the bond to sample nearly all of the conformational space that would be available to the glycosidic bonds in a linear β-(1 → 2)-linked glucan. The average geometry of the bond depends not only on the range of conformational space available to it, but also on the amount of time it spends in each of the conformational states that it samples. Thus, the precise nature and extent of the constraints imposed by the cyclization of α-C16 cannot be assumed a priori. Nevertheless, these constraints may favor conformations that have a common geometric pattern, thus making it possible to use parameters measured by NMR spectroscopy to derive a realistic conformational model for α-C16.

Several conformational models for cyclic β-(1 → 2)-glucans have been developed, all of which attempt to reconcile the tendency for individual glycosidic bonds to adopt energetically favorable conformations with the requirement for closure of the macrocyclic ring. An energetically favorable glycosidic bond conformation theoretically corresponds to residence in a well in the energy surface calculated as a function of various geometric parameters. The calculated energy surface plotted as a function of the glycosidic torsional angles ϕ and ψ of β-sophorose is shown in Fig. 6. This surface was obtained by analysis of a Monte Carlo simulation calculated using a relatively simple "HSEA" force field [23]. Although this type of calculation often overestimates the energies of sterically crowded conformations such as transition states, it provides energy surfaces that agree qualitatively with the energy surfaces provided by more realistic calculations. For example, the three main wells in the energy surface for β-sophorose calculated [10] using MM3 span regions of the ϕ,ψ map that are qualitatively similar to those covered by the three energy wells (labeled A, B, and C in Fig. 6) calculated using the HSEA method. A β-(1 → 2)-linked glucosidic bond can thus be classified as having conformation A, B, or C, according to its residence in one of these three energy wells.

Most of the different conformational models proposed for the cyclic β-(1 → 2)-glucans are based on the residence of glycosidic bonds in one or more of the three energy wells described above. An exception is the model of Serrano et al. [8], who proposed that glycosidic bond geometry alternates between conformation A and a second conformation ($\phi = 165 \pm 8$, $\psi = 180 \pm 8$) that has been rejected as energetically unfavorable in other studies [7,10]. The model of Palleschi and Crescenzi [6] consists of a tandemly repeated series of trisaccharide conformational repeat units, with all glycosidic bonds in the most favorable conformation A. An alternative model, based on cluster analysis of Monte Carlo simulations [7], consists of a series of either tetrasaccharide or heptasaccharide conformational repeat units in which one of the glycosidic bonds in the repeat unit adopts conformation B and all other bonds adopt conformation A. It has been difficult to obtain experimental evidence to confirm or refute these models

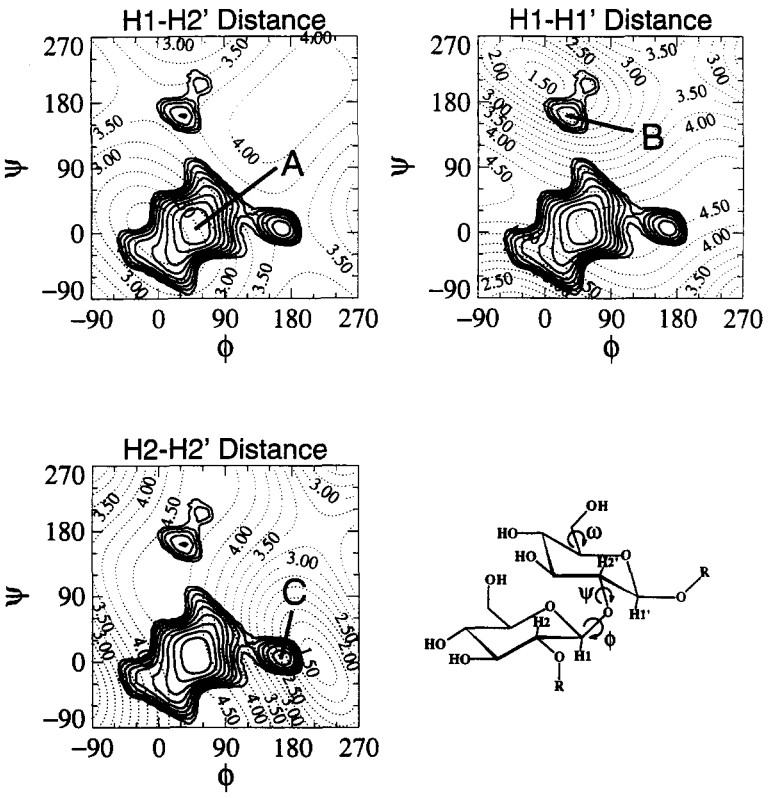

Fig. 6. Interproton distance maps (dotted lines) overlaid with the conformational energy map (solid lines) for β-sophorose. The dihedral angles ϕ (H-1–C-1–O-2′–C-2′), ψ (C-1–O-2′–C-2′–H-2′), and ω (O-6–C-6–C-5–H-5) are indicated in the β-sophorose structure drawn at the lower right. The conformational energy map was obtained by analysis of a Monte Carlo simulation performed using the GEGOP program, utilizing an HSEA-type force field, with energy contours drawn at 1 kcal/mol intervals. Interproton distances were calculated as a function of the dihedral angles ϕ and ψ using the same rigid $^4C_1$ sugar geometry as was utilized during the HSEA calculations. The distance map for a specific pair of protons is shown in each panel, and the energy well corresponding to a small interproton distance for that pair is indicated by the uppercase letter in each panel. The geometry of a given β-(1 → 2) glycosidic bond is classified according to its residence in one of the energy wells indicated by these uppercase letters as conformation A, B, or C. Conformations $^+$A and $^-$A correspond to residence in one or two subregions of energy well A, distinguished principally by the value of ψ (i.e., $\psi > -20$ for $^+$A and $\psi < -20$ for $^-$A).

because conformational averaging prevents the geometric analysis of individual glycosidic bonds within the Rhizobiaceae cyclosophorans.

The chemical shift dispersion of the H-1 and H-2 resonances of α-C16 makes it possible to probe the geometries of specific, individual glycosidic bonds within this unique molecule. For example, residence of a glycosidic bond in one of the energy wells described above would bring a specific pair of protons into close proximity, and detection of the resulting NOE would therefore provide evidence that a particular conformation had been adopted by the glycosidic bond. This is illustrated for the

β-(1 → 2) linkage of β-sophorose in Fig. 6, in which isometric contour lines for several internuclear distances that depend on the torsional angles ϕ and ψ are plotted along with the calculated (HSEA) conformational energy surface. These calculations indicate that glycosidic bonds in conformation A would exhibit a strong H-1–H-2′ NOE, those in conformation B would exhibit a strong H-1–H-1′ NOE, and those in conformation C would exhibit a strong H-2–H-2′ NOE. A strong H-1–H-2′ NOE is observed for every β-(1 → 2) glycosidic bond of α-C16, indicating that each of its β-(1 → 2) glycosidic bonds adopts the A conformation, at least transiently. In contrast, no H-1–H-1′ or H-2–H-2′ cross-peaks were observed in the NOESY spectrum of α-C16, indicating that none of its β-(1 → 2) glycosidic bonds is permanently trapped in either the B or C conformation. It is possible that the B and C conformations are transiently adopted, but that these conformational states have no observable effect on the NOESY spectrum because they are diluted by conformational averaging in α-C16. However, these results are most simply explained by the hypothesis that α-C16 readily adopts molecular geometries wherein all of its β-(1 → 2) glycosidic bonds are simultaneously in the A conformation.

An alternating pattern becomes apparent when the chemical shift of the H-1, H-2, C-1, and C-2 resonances of α-C16 are plotted (Fig. 7A and B) as a function of the glycosidic bond position with respect to the α-(1 → 6)-linkage, implying that the average conformation of glycosidic bonds in α-C16 is also alternating. This is consistent with previous studies [27,28] of β-linked glucosides which indicated that changes in the dihedral angles ϕ and ψ affect the chemical shifts of the anomeric carbon (C-1) and the aglyconic carbon [i.e., C-2′ in the case of a β-(1 → 2) linkage]. For example, the C-1 (δ 104.9) and C-2 (δ 84.9) resonances of a crystalline form of cellobiose, wherein the dihedral angles are frozen at ($\phi = 44$, $\psi = 12$), are upfield of the corresponding C-1 (δ 106.5) and C-2 (δ 85.5) resonances in a crystalline form of methyl β-cellobioside, wherein the dihedral angles are frozen at ($\phi = 29$, $\psi = -41$) [27]. The transition between these two conformations involves a large change in ψ and a smaller change in ϕ, which presumably is constrained by the exo-anomeric effect [27]. Furthermore, these conformations are analogous to two local minima ($\phi = 48.0$, $\psi = -8.3$ and $\phi = 34.0$, $\psi = -43.4$) in the deepest (conformation A) energy well of the MM3 energy surface calculated for β-sophorose by Dowd et al. [10]. These observations are consistent with the hypothesis that systematic variations in the chemical shifts of the C-1 and C-2 resonances of α-C16 correspond to systematic variations in the average values of ϕ and ψ.

Conformational models of β-(1 → 2)-linked glucans were generated based on the observations outlined in the preceding paragraph. Initially, the energy well corresponding to conformation A was arbitrarily divided into two subregions that are distinguished by the dihedral angle ψ. The region of the energy well wherein $\psi > -20$ was defined as conformation $^{+}$A and was associated with ^{13}C resonances that were shifted upfield in the alternating pattern shown in Fig. 7B. The region wherein $\psi < -20$ was defined as conformation $^{-}$A and was associated with ^{13}C resonances that were shifted downfield in this alternating pattern. A linear β-(1 → 2)-linked tridecaglucoside takes the form of a ribbon-like right-handed helix (Fig. 8A, conformation I in Table 3) when the glycosidic bond geometry alternates between the $^{+}$A and $^{-}$A conformations. This conformation

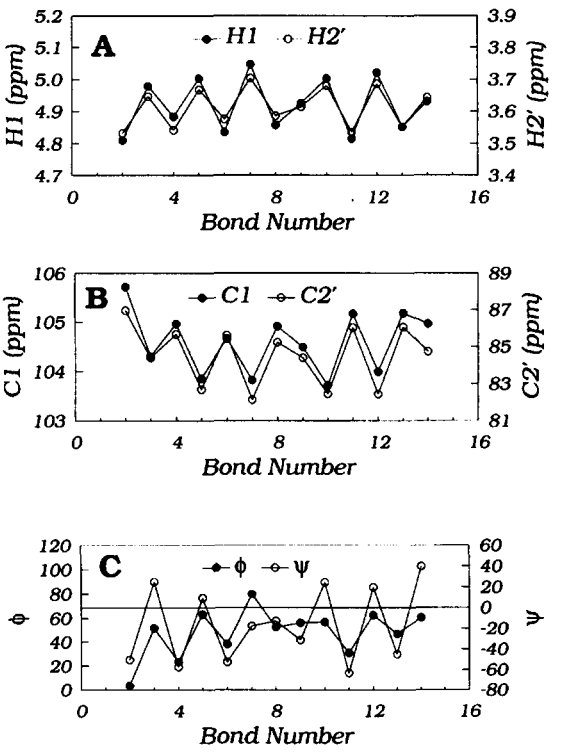

Fig. 7. Dependence of the ^{1}H NMR chemical shifts (panel A) and ^{13}C NMR chemical shifts (panel B) on the location of the nucleus within α-C16. Bond number N corresponds to the glycosidic linkage between Glc*p* residues N and N+1 (Fig. 1), and so the chemical shifts of the H-1 and C-1 resonances for residue N and the chemical shifts of the H-2′ and C-2′ resonances for residue N+1 are associated with bond N. Cyclization makes Bond 0 (i.e., the α-(1 → 6) linkage between residues **16** and **1**, see Fig. 1) equivalent to Bond 16. The alternating pattern of chemical shifts undergoes a "frame shift" at Bonds 8–10. This frame shift hypothetically leads to a reversal of helix topology in the glucan, as illustrated in Fig. 8. Panel C illustrates the alternating pattern of glycosidic dihedral angles in conformation III (Table 3, Fig. 8C).

may be stabilized by the formation of hydrogen bonds. That is, even-numbered residues of a β-(1 → 2) glucan in this conformation could form an extended hydrogen-bond network along one edge of the ribbon, and odd-numbered residues could form a similar hydrogen-bond network along the other edge.

Closer examination of the chemical shift pattern for H-1, H-2, C-1, and C-2 of α-C16 (Fig. 7) reveals that it is not strictly alternating, because the chemical shifts of nuclei associated with glycosidic bonds **9** and **10** are roughly equivalent, leading to a "frame shift" for the pattern. A β-(1 → 2)-linked tridecaglucoside (Fig. 8B, conformation II in Table 3) that embodies two such alternating $^{+}A/^{-}A$ patterns connected via a frame shift exhibits a reversal of helix topology at the point of the frame shift. Such a reversal of helix topology can bring the reducing and nonreducing terminal residues of a β-(1 → 2)-linked glucan containing 16 residues into close proximity, allowing cyclization to occur via an α-(1 → 6)-glycosidic bond (Fig. 8C, conformation III in Table 3).

Table 3
Parameters for selected conformational states [a]

Bond [d]	Conformation [a] I Linear 13 Residues Minimized [b] 44.4 kcal/mol		Conformation [a] II Linear 13 Residues Minimized [b] 41.2 kcal/mol		Conformation [a] III α-C16 16 Residues Minimized [b] 36.7 kcal/mol		Conformation [a] IV α-C16 16 Residues Annealed [c] 21.2 kcal/mol		Conformation [a] V Cyclic, All β 18 Residues Minimized [b] 53.8 kcal/mol		Conformation [a] VI Cyclic, All β 18 Residues Annealed [c] 25.4 kcal/mol	
	ϕ	ψ	ϕ	ψ	ϕ	ψ	ϕ	ψ	ϕ	ψ	ϕ	ψ
1	11.9	−48.3	55.0	17.9	71.2	61.5	71.1	62.0	28.9	−52.7	29.0	−58.4
2	48.6	30.2	27.3	−54.6	3.5	−50.5	−22.6	−39.2	56.4	13.6	68.3	2.8
3	19.0	−49.1	54.2	17.4	51.7	25.0	39.4	27.2	24.7	−60.1	29.7	−59.2
4	47.6	29.8	21.9	−56.9	23.8	−57.4	24.1	−57.1	54.4	20.5	61.9	10.5
5	20.3	−50.5	60.6	10.5	63.2	9.3	76.5	−9.5	29.7	−55.1	20.8	−53.6
6	48.0	29.7	25.8	18.8	38.3	−52.7	43.5	−73.1	54.6	17.3	56.6	20.8
7	20.3	−50.8	32.1	−61.7	79.7	−17.7	92.4	−34.0	22.6	−56.4	12.9	−48.1
8	48.2	29.1	58.9	12.4	52.5	−12.9	65.6	−12.7	61.8	9.6	71.3	−20.9
9	20.2	−51.6	27.4	−57.1	56.0	−31.4	58.3	−19.7	32.1	16.0	42.1	27.6
10	48.8	26.3	55.4	18.3	56.9	24.4	56.4	30.8	36.3	−65.2	−5.9	−53.6
11	19.1	−56.0	28.4	−55.5	30.9	−63.4	−12.3	−40.2	60.8	12.2	48.7	17.3
12	53.0	28.1	55.4	21.6	62.5	19.4	50.9	0.7	27.4	−56.9	34.4	−48.0
13					46.9	−45.1	48.1	−54.8	55.7	19.2	63.7	−5.5
14					60.3	39.7	71.5	61.6	31.1	−55.3	32.3	−56.7
15					49.8	28.3	58.3	48.3	54.1	18.7	68.2	5.4
16					−64.1 [e]	175.7 [e] (15.4) [e]	64.3 [e]	167.2 [e] (48.7) [e]	19.5	−57.3	33.0	−59.1
17									55.7	21.9	128.2	−48.8
18									4.5	36.4	62.4	7.8

[a] See Fig. 8 for conformations I, II, III, and V. Conformations IV and VI are are less symmetrical annealed forms of II and V, respectively, and are not depicted in Fig. 8.
[b] Conformation after energy minimization.
[c] Conformation after simulated annealing and energy minmimization.
[d] Bond 1 refers to the bond between residues **1** and **2**, where residue numbers increase toward the reducing end, as in Fig. 1.
[e] Bond 16 of α-C16 is the α-(1 → 6)-linkage between residues **16** and **1**; in this case ψ is defined C-1–O-6′–C-6′–C-5′, and ω (in parentheses) is O-6′–C-6′–C-5′–H-5′.

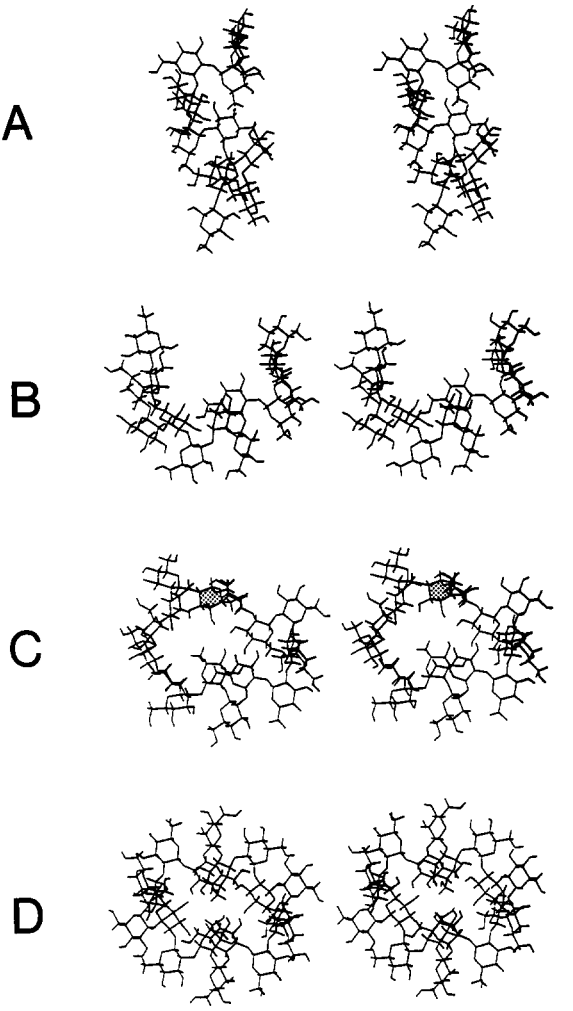

Fig. 8. Stereoimages of conformational models for β-(1 → 2)-linked glucans. (A) Tridecasaccharide (Table 3, conformation I) with a sequence of strictly alternating ($^{-}$A/$^{+}$A) glycosidic bond conformations, leading to a ribbon-like right-handed helix. (B) Tridecasaccharide (Table 3, conformation II) with two sequences of alternating ($^{-}$A/$^{+}$A) glycosidic bond conformations connected via a "frame shift", leading to a reversal of helix topology at the point of the frame shift. (C) Idealized conformation (Table 3, conformation III) of α-C16 that embodies two sequences of alternating ($^{-}$A/$^{+}$A) glycosidic bond conformations. A frame shift in the sequence of β-(1 → 2) glycosidic bond conformations and the α-(1 → 6) linkage provide the two topological reversal points that are necessary for cyclization. The α-Glc*p* residue is shaded. (D) Idealized conformation (Table 3, conformation V) for a cyclic β-glucan composed of 18 β-(1 → 2)-linked Glc*p* residues with no α-(1 → 6) linkage. Both topological reversal points are provided by frame shifts in the sequence of β-(1 → 2) glycosidic bond conformations. The model is viewed along the C_2 axis of symmetry.

The alternating dihedral angle pattern for conformation III (Fig. 7C) corresponds quite well to the alternating chemical shift pattern (Fig. 7A and B) for α-C16. Conformation III consists of two helical domains that must be joined via two topological reversal

points in order for cyclization to occur. One of these topological reversal points occurs at a frame shift in the alternating $^{+}A/^{-}A$ pattern and the other occurs at the flexible α-(1 → 6)-linkage. Many conformational states that have this general pattern of glycosidic bond geometry are possible. One such state (conformation IV, Table 3) was obtained by simulated annealing of conformation III (Table 3, Fig. 8C).

The frame-shifted, alternating $^{+}A/^{-}A$ conformational pattern can also lead to cyclization of β-(1 → 2)-glucans that do not have an α-(1 → 6) linkage. The cyclic β-glucans produced by the Rhizobiaceae lack α-(1 → 6) linkages, and invariably have at least 17 β-Glc*p* residues [2]. This suggests that two or more (1 → 2)-linked β-Glc*p* residues in the Rhizobiaceae glucans can substitute for the (1 → 6)-linked β-Glc*p* residue in α-C16, providing the second topological reversal site that is required for closure of the macrocycle. Thus, the conformational model for α-C16 can be extended to the Rhizobiaceae glucans by including two symmetrically located frame shifts in the $^{+}A/^{-}A$ conformational pattern (Fig. 8D, conformation V in Table 3). Conformation VI (Table 3) was obtained by simulated annealing of conformation V.

The conformational states described in Table 3 were generated by observing the conformational effects of manually changing various dihedral angles in the glucan. The sterically accessible conformations that resulted from this somewhat arbitrary procedure are representative of the proposed model, but are not necessarily the conformations with the minimum energy. Nevertheless, the calculated energies of these conformations are similar to those calculated for conformations representing the previously proposed models [7]. A theoretical comparison of the energetics of the different conformational models would require very extensive (and computationally expensive) simulations that take into account effects not explicitly addressed in the relatively simple calculations described herein. Nevertheless, these simple calculations indicate that the molecular geometries predicted by the proposed conformational model are sterically accessible.

A high degree of symmetry was incorporated into the idealized forms (Fig. 8C and D, Table 3, conformations III and V) as a matter of convenience during their generation, but high symmetry does not necessarily correspond to low energy. The annealed forms (Table 3, conformations IV and VI) are less symmetrical, and although they are thus less representative of the canonical model, they each represent only one of many possible subtle variations that are likely to occur for an actual cyclic glucan in solution. For example, one or two of the glycosidic bonds in conformations IV and VI (Table 3) are not within the deepest part of the main energy well corresponding to conformation A, but in no case do these excursions lead to close H-1–H-1′ or H-2–H-2′ contacts, in keeping with the experimental evidence described above.

The proposed conformational model correctly predicts the general features of the NMR spectra of the cyclosophorans produced by Rhizobiaceae. The point of reversal in helix topology that occurs when two consecutive β-(1 → 2)-linkages adopt similar conformations can easily migrate along the glucan chain. That is, each step in the conformational transformation $\{\ldots {}^{+}A^{-}A^{-}A^{+}A^{-}A^{+}A\ldots\}$ to $\{\ldots {}^{+}A^{-}A^{+}A^{+}A^{-}A {}^{+}A\ldots\}$ and then to $\{\ldots {}^{+}A^{-}A^{+}A^{-}A^{-}A^{+}A\ldots\}$ is a low-energy process, requiring only a molecular translation or rotation coupled to a shift in the geometry of one glycosidic bond via a low-energy transition state. In a cyclic glucan containing *only* β-(1 → 2)-linkages, this transformation would result in the migration of the topological

reversal points around the ring. It is likely that such a process would occur rapidly on the NMR time scale, exposing each of the β-Glc*p* residues of the molecule to the same average magnetic environment, and leading to the signal degeneracy that is observed in the NMR spectra of these glucans.

In contrast, the position of the α-(1 → 6)-linkage in α-C16 is chemically fixed. The proposed conformational model for α-C16 is consistent with the observed alternating chemical shift pattern if one assumes that the α-(1 → 6) linkage forms one of the topological reversal points in the lowest energy (and therefore most populated) α-C16 conformations, thus restricting the second topological reversal point in these low-energy conformations to bonds 8–10. In this scenario, other higher-energy α-C16 conformations could be formed by migration of the topological reversal points, but those conformers would not contribute significantly to the ensemble average conformation due to their low population and transient nature. The general model described above thus provides a simple mechanism to explain the spectroscopic properties of all known types of cyclic β-(1 → 2)-linked glucans.

4. Conclusions

Analyses of the NMR spectra of α-C16 are consistent with the hypothesis that α-C16 is more conformationally constrained than linear β-(1 → 2)-linked glucans. The combination of this putative conformational constraint and the ability to distinguish the NMR resonances of each Glc*p* residue in α-C16 make this cyclic glucan a very attractive model system for studying the relationships between glycosidic bond geometry and several NMR parameters, including heteronuclear scalar coupling constants and ^{1}H and ^{13}C chemical shifts. Assignment of the NMR spectra of α-C16 reveals an alternating pattern in the chemical shifts of the H-1, H-2, C-1, and C-2 resonances of the β-Glc*p* residues. This alternating pattern can be interpreted in terms of a general conformational model for cyclic β-(1 → 2)-linked glucans, which in turn suggests a simple mechanism for the conformational averaging that is observed in the cyclosophorans produced by the Rhizobiaceae.

Acknowledgements

This research is supported by United States Department of Energy (DOE) grant DE-FG05-93ER20115, and by the DOE-funded (DE-FG05-93ER20097) Center for Plant and Microbial Complex Carbohydrates. W.S.Y. thanks Drs Alan Darvill and Peter Albersheim, Directors of the CCRC, for their continuing support, Stephen Hantus, Joe Silva, Lisa K. Harvey and Dr Parastoo Azadi for technical assistance, Karen Howard for help with preparing the manuscript, Dr Russell Carlson for providing mixtures of *R. trifolii* cyclosophorans and for helpful discussions, Dr Mark Schell for providing the strain of *Xanthomonas campestris*, Dennis Warrenfeltz for maintenance of the spectrometers, and Drs Robert J. Woods, Jan U. Thomsen, John Glushka and Sandeep Kalelkar for enlightening discussions.

References

[1] K.J. Miller, E.P. Kennedy, and V.N. Reinhold, *Science*, 231 (1986) 48–51.
[2] M.W. Breedveld and K.J. Miller, *Microbiol. Rev.*, 58 (1994) 145–161.
[3] K. Koizumi, Y. Okada, U. Horiyama, T. Utamura, M. Hisamatsu, and A. Amemura, *J. Chromatogr.*, 299 (1984) 215–224.
[4] A. Dell, W.S. York, M. McNeil, A.G. Darvill, and P. Albersheim, *Carbohydr. Res.*, 117 (1983) 185–200.
[5] A. Amemura and J. Cabrera-Crespo, *J. Gen. Microbiol.*, 132 (1986) 2443–2452.
[6] A. Palleschi and V. Crescenzi, *Gazz. Chim. Ital.*, 115 (1985) 243–245.
[7] W.S. York, J.U. Thomsen, and B. Meyer, *Carbohydr. Res.*, 248 (1993) 55–80.
[8] A.M. Gil Serrano, G. Franco-Rodriguez, I. Gonzalez-Jimenez, P. Tejero-Mateo, J.M. Molina, J.A. Dobado, M. Megias, and M.J. Romero, *J. Mol. Struct.*, 301 (1993) 211–226.
[9] D.A. Cumming and J.P. Carver, *Biochemistry*, 26 (1987) 6664–6676.
[10] M.K. Dowd, A.D. French, and P.J. Reilly, *Carbohydr. Res.*, 233 (1992) 15–34.
[11] Y. Inoue, *Annu. Rep. NMR Spectrosc.*, 27 (1993) 59–101.
[12] T. Steiner and W. Saenger, *Carbohydr. Res.*, 259 (1994) 1–12.
[13] L. Poppe, W.S. York, and H. van Halbeek, *J. Biol. NMR*, 3 (1993) 81–89.
[14] R.K. Harris, *Nuclear Magnetic Resonance Spectroscopy*, Pitman, Marshfield, Mississippi, 1983.
[15] T. Higashiura, M. Ikeda, M. Okubo, M. Hisamatsu, A. Amemura, and T. Harada, *Agric. Biol. Chem.*, 49 (1985) 1865–1866.
[16] M. Rance, O.W. Sorensen, G. Bodenhausen, G. Wagner, R.R. Ernst, and K. Wuthrich, *Biochem. Biophys. Res. Commun.*, 117 (1983) 479–485.
[17] A. Bax and D.G. Davis, *J. Magn. Reson.*, 65 (1985) 55–360.
[18] M. Rance, G. Bodenhausen, G. Wagner, K. Wuthrich, and R.R. Ernst, *J. Magn. Reson.*, 62 (1985) 497–510.
[19] G. Bodenhausen and D.J. Ruben, *Chem. Phys. Lett.*, 69 (1980) 185–189.
[20] T.J. Norwood, J. Boyd, J.E. Heritage, N. Soffe, and I.D. Campbell, *J. Magn. Reson.*, 87 (1990) 488–501.
[21] D. Marion and K. Wuthrich, *Biochem. Biophys. Res. Commun.*, 113 (1983) 967–974.
[22] A.J. Shaka, P.B. Barker, and R. Freeman, *J. Magn. Reson.*, 64 (1985) 547–552.
[23] R. Stuike-Prill and B. Meyer, *Eur. J. Biochem.*, 194 (1990) 903–919.
[24] M. Hisamatsu, W.S. York, A.G. Darvill, and P. Albersheim, *Carbohydr. Res.*, 227 (1992) 45–71.
[25] K. Bock and H. Pedersen, *J. Carbohydr. Chem.*, 3 (1984) 581–592.
[26] W.S. York, P. Albersheim, and A.G. Darvill, unpublished results.
[27] M.C. Jarvis, *Carbohydr. Res.*, 259 (1994) 311–318.
[28] A.S. Shashkov, G.M. Lipkind, Y.A. Knirel, and N.K. Kochetkov, *Magn. Reson. Chem.*, 26 (1988) 735–747.